Cell and Tissue Research (2019) 376:471–484
https://doi.org/10.1007/s00441-019-02999-8

REGULAR ARTICLE

Distribution of neuropeptide F in the ventral nerve cord and its possible role on testicular development and germ cell proliferation in the giant freshwater prawn, *Macrobrachium rosenbergii*

Sirorat Thongrod[1] · Chaitip Wanichanon[1] · Prasert Sobhon[1,2]

Received: 26 April 2018 / Accepted: 21 January 2019 / Published online: 19 February 2019

Abstract

Neuropeptide F in invertebrates is a homolog of neuropeptide Y in mammals and it is a member of FMRFamide-related peptides. In arthropods, such as insects, there are two types of neuropeptide F comprising long neuropeptide F (NPF) and short neuropeptide F (sNPF). Both NPFs are known to play a crucial role in the regulations of foraging, feeding-related behaviors, circadian rhythm, stress responses, aggression and reproduction in invertebrates. We have earlier found that in the giant freshwater prawn, *Macrobrachium rosenbergii*, there are three isoforms of NPF and four isoforms of sNPF and that NPFs are expressed in the eyestalks and brain. In the present study, we investigate further the tissue distribution of NPF-I in the ventral nerve cord (VNC) and its role in the development of testes in small male (SM) *Macrobrachium rosenbergii*. By immunolocalization, using the rabbit polyclonal antibody against NPF-I as a probe, we could detect NPF-I immunoreactivity in the neuropils and neuronal clusters of the subesophageal ganglia (SEG), thoracic ganglia (TG) and abdominal ganglia (AG) of the SM prawns. In functional assays, the administrations of synthetic NPF-I (KPDPTQLAAMADALKYLQELDKYYSQVSRPRFamide) and sNPF (APALRLRFamide) peptides significantly increased the growth rates of SM prawns and significantly increased the gonadosomatic index (GSI) and proliferations of early germ cells in the seminiferous tubules of their testes. It is, therefore, suggestive that NPFs may play critical roles in energy homeostasis towards promoting growth as well as testicular development in prawns that could be applied in the aquaculture of this species.

Keywords Neuropeptide F · Ventral nerve cord · Subesophageal ganglion · Testis · *Macrobrachium rosenbergii*

Introduction

The giant freshwater prawn, *Macrobrachium rosenbergii*, is an important commercial prawn species that is widely distributed in the tropical and subtropical zones of the Indo-Pacific region, including India, Australia, Malaysia, Indonesia, Philippines and Thailand. The demand for giant freshwater prawns is high; thus, aquaculture is the main source of production like in cases of penaeid shrimps and is comparable in terms of commercial prospects. In contrast to penaeid shrimps, the male giant freshwater prawns are much larger than the females, especially when they are fully grown at 6 months (Rungsin et al. 2006). Therefore, farmers want large and fast-growing male stocks that can fetch a higher price. Despite the development of appropriate feed that can promote fast growth, addition or administration of feed-stimulating and growth-promoting substances, such as neuropeptide F, could be another means to help achieve this goal.

nvertebrate neuropeptide F (NPF) is a homolog of neuropeptide Y (NPY) of vertebrates and it is a member of the FMRFamide-related peptides. In arthropods, it has been extensively studied in *Drosophila*. There are two types of neuropeptide F: the so-called long neuropeptide F (NPF) that consists of two isoforms, NPF-I and NPF-II, arising from a duplication of a single gene and a short NPF (sNPF) comprising four isoforms arising from the splicing within a single gene (Carlsson et al. 2013). Both NPFs and sNPF play crucial roles in the regulation of foraging, feeding, growth, circadian rhythm, stress responses and aggression in insects (Karl and

✉ Prasert Sobhon
prasert.sob@mahidol.ac.th

[1] Department of Anatomy, Faculty of Sciences, Mahidol University, Rachathewi, Bangkok 10400, Thailand

[2] Faculty of Allied Health Sciences, Burapha University, Long-Hard Road, Bangsaen, Mueang District, Saen Suk, Chonburi 20131, Thailand

Herzog 2007; Nassel and Wegener 2011). In crustaceans, NPFs were first identified in the penaeid shrimp, *Litopenaeus vannamei* (Christie et al. 2008, 2011) and in *Daphnia pulex* (Gard et al. 2009) by transcriptomic analyses. Recently, our group reported on the identity, expression and ovarian-stimulating activity of NPF in freshwater prawns. Through the analyses of the central nervous system (CNS) and gonad transcriptomes, we found that there are three isoforms of long NPF and four isoforms of short NPF (Suwansa-Ard et al. 2015). Subsequently, Mro-NPF-I and Mro-NPF-II were characterized by reverse transcription polymerase chain reaction (RT-PCR) to have 32-amino-acid and 69-amino-acid active peptides, respectively, with identical sequences except for the middle insert of 37 amino acids. Mro-NPF-I was found to be the major isoform being expressed in neuropils and neuronal clusters in the eyestalk and brain of male prawns (Thongrod et al. 2017). The two forms of crustacean NPFs as reported by our group and Christie et al. (2008, 2011) correspond to NPF1a and NPF1b of some insects (Roller et al. 2008). Recently, through a functional assay, we found that Mro-NPF-I (KPDPTQLAAMADALKYLQELDKYY SQVSRPRFamide) could stimulate ovarian development in the female prawns (Tinikul et al. 2017). Therefore, the aims of this study are to further localize the Mro-NPF-I expression in the ventral nerve cord (VNC) to obtain the complete picture of NPF tissue expression in the central nervous system (CNS) of the prawn and to investigate the effects of Mro-NPF-I and Mro-sNPF (APALRLRFamide) on growth and testicular development in the male giant freshwater prawns.

Materials and methods

Experimental animals

Small male (SM) giant freshwater prawns, *M. rosenbergii*, with a body weight of 30 ± 5 g, were purchased from a local farm in Suphanburi Province, Thailand. They were maintained in rectangular plastic tanks at the Department of Anatomy, Faculty of Science, Mahidol University. The prawns were kept under a photoperiod of 12:12-h light–dark with continuous aeration and fed with commercial pellets (Sunshine, Bangkok, Thailand) once a day for 1 week before treatments. All the treatment protocols were carried out according to the guidelines set by the Ethic Committee on the Use of Experimental Animals, Faculty of Science, Mahidol University.

Immunofluorescence detection of Mro-NPF-I in the ventral nerve cord

Subesophageal, thoracic and abdominal ganglia, which are the main parts of the ventral nerve cord, were collected and fixed with 4% paraformaldehyde for 24 h at 4 °C. The fixed tissues were dehydrated in a series of ethanol (70%, 80%, 90%, 95% and 100% for 1 h each), then immersed in xylene, infiltrated with paraffin and finally embedded in paraffin blocks. The embedded tissues were cut at a thickness of 5 μm by a rotary microtome (Leica RM2235, Germany) and the sections were mounted on slides coated with 3-aminopropyltriethoxy-silane solution (Sigma, St. Louis, Mo., USA) and dried at 37 °C overnight. The tissue sections were deparaffinized in xylene, rehydrated through a graded series of ethanol, equilibrated in PBS, then permeabilized in 0.4% Triton X-100 in PBS and blocked from non-specific binding in 5% normal goat serum (NGS) in PBST for 1 h at room temperature. The sections were incubated with rabbit polyclonal antibodies against Mro-NPF-I (anti-Mro-NPF-I) (produced and tested for specificity as mentioned in Thongrod et al. 2017 and verified further by Western blot as shown in Fig. 1) at a dilution of 1:500 in PBS at 4 °C for 24 h. Then, they were washed extensively in 0.4% PBST and incubated in Alexa 488–conjugated goat anti-rabbit IgG (Molecular Probes, Eugene, Ore., USA) diluted at 1:500 in the blocking solution for 1 h. TO-PRO-3 (Molecular Probes, Invitrogen, USA) was used at a 1:3000 dilution for nuclear staining. The sections were examined and images were taken with an Olympus FV3000 confocal laser scanning microscope.

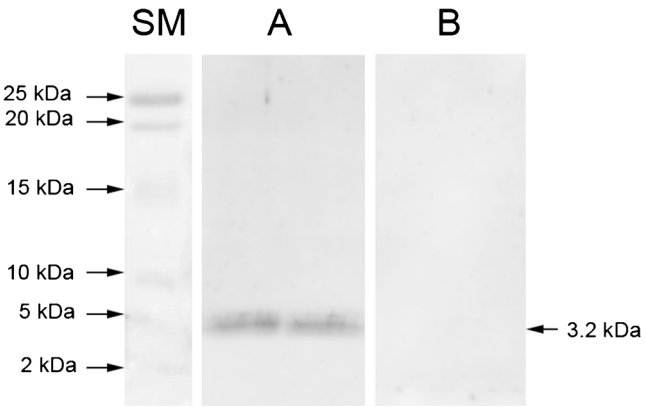

Fig. 1 **a** To demonstrate Mro-NPF antibody specificity, the Mro-NPF protein (15 μg per lane) was run in a 15% SDS–PAGE and transferred onto 0.45-μm nitrocellulose membranes (GE Healthcare Bio-Sciences). The membrane with transferred protein was blocked from non-specific bindings by incubating with 5% skim milk in PBS for 1 h at room temperature. Then, it was incubated with anti-Mro-NPF at 1:500 dilution at 4 °C for overnight. Next, the membrane was incubated with anti-rabbit IgG coupled to HRP at a dilution of 1:5000 for 2 h at room temperature. Immunoreactive band was revealed by using a chemiluminescence detection kit (Amersham Pharmacia Biotech, Buckinghamshire, UK) and detected with an ImageQuant LAS 500 (GE Healthcare Bio-Sciences). The band appearing on a Western blot at 3.2 kDa indicates specific binding between the Mro-NPF protein and Mro-NPF antibody. **b** For negative control, a membrane containing the transferred Mro-NPF protein prepared as stated in **a** was incubated with the primary antibody preabsorbed with Mro-NPF peptide and the membrane was incubated with anti-rabbit IgG coupled to HRP at a dilution of 1:5000 for 2 h at room temperature, then washed extensively with 0.2% Tween in PBS (0.2% PBST). The membrane shows no immunoreactive band that firmly demonstrates the specificity of Mro-NPF antibody (SM: standard marker)

Immunoperoxidase detection of Mro-NPF-I in the ventral nerve cord

Subesophageal, thoracic and abdominal ganglia were collected and fixed with 4% paraformaldehyde for 24 h at 4 °C. The fixed tissues were dehydrated in a series of ethanol (70%, 80%, 90%, 95% and 100% for 1 h each). The tissues were immersed in xylene, infiltrated with paraffin and embedded in paraffin blocks. The embedded tissues were cut at a thickness of 5 μm on a rotary microtome (Leica RM2235, Germany) and the sections were mounted on slides coated with 3-aminopropyltriethoxy-silane solution (Sigma, St. Louis, Mo., USA) at 37 °C overnight. Rehydrated sections were immersed in 10 mM citrate buffer, pH 6.0 and then endogenous peroxidase and free aldehyde groups were blocked by immersing the sections in 3% H_2O_2 in methanol and in 1% glycine in 0.1 M PBS. Subsequently, the sections were incubated in the blocking solution of 5% normal goat serum (NGS) in PBST to block nonspecific binding. The sections were subsequently incubated with anti-Mro-NPF-I diluted at 1:500 at 4 °C overnight, followed by the secondary antibody, i.e., HRP-conjugated goat anti-rabbit IgG (SouthernBiotech, Birmingham, USA), at a 1:2000 dilution for 2 h. The immunoreactivity (−ir) was detected by immersing tissue sections in NovaRED substrate (Vector Laboratory, Burlingame, Calif., USA) until a red color was observed. Finally, the sections were mounted in 90% glycerol in PBS, observed under a Nikon E600 light microscope and photographed by a Nikon DXM 1200E digital camera (Japan).

Effect of NPF injections on growth and testicular development

The Mro-NPF-I (KPDPTQLAAMADALKYLQELDKYY SQVSRPRFamide) and Mro-sNPF (APALRLRFamide) peptides (whose sequences were determined by Suwansa-ard et al. 2015) were custom synthesized by GenScript (Piscataway, N.J., USA). In the functional assays for testing the effects of NPF injections on growth and testicular development, small male prawns were divided into 5 groups of 45 animals each: prawns in the first group were injected with 100 μl of 0.1 M PBS; prawns in the second group were injected with Mro-NPF-I at 2.5×10^{-6} mol/prawn; prawns in the third group were injected with Mro-NPF-I 2.5×10^{-7} mol/prawn; prawns in the fourth group were injected with Mro-sNPF 2.5×10^{-6} mol/prawn; and prawns in the last group were injected with Mro-sNPF 2.5×10^{-7} mol/prawn. Each NPF injection was delivered in 100 μl of 0.1 M PBS and each treated prawn was injected at days 0, 4, 8 and 12, while the control prawns were injected with PBS at the same volume at the same intervals. Then, they were placed in rectangular tanks to rest and feed. The prawns ($N = 6$) were sacrificed and the testes were collected and fixed with 4% paraformaldehyde every 4 days until day 28 starting from day 4. Body weights and testicular weights were measured and gonadosomatic indexes (GSI = testicular weight/body weight × 100) were calculated.

Determination of germ cell proliferation by BrdU labeling of dividing cells

To investigate and estimate cellular proliferation in the testes of control and treated prawns, each male was injected with 5 mg of 5-bromo-2′-deoxyuridine (BrdU) per 100 g of body weight dissolved in distilled water, 6 h prior to sacrifice. The sections of testes of BrdU-injected prawns ($N = 6$) were used for determining the amount of BrdU-positive cells by immunolabeling as described in Detection Kit II (Roche, Mannheim, Germany). Briefly, the sections were deparaffinized and rehydrated. Then, they were treated with 0.01 M citrate buffer, pH 6.0, in a microwave oven at 700 W for 15 min 3 times and incubated with 2 M HCl at 37 °C for 1 h. The sections were washed in 0.1 M PBS and treated with 1% glycine in 0.1 M PBS at room temperature for 15 min. They were washed again and then incubated in the blocking solution (4% bovine serum albumin (BSA) in 0.1 M PBS) for 1 h. The sections were incubated with anti-BrdU (mouse monoclonal antibody, diluted 1:20 with 1% BSA in 0.1 M PBS), at 4 °C overnight. Then, they were washed and incubated with anti-mouse IgG linked to alkaline phosphatase (AP) (SouthernBiotech, Birmingham, USA) (1:500 diluted with 1% BSA in 0.1 M PBS), at 37 °C for 2 h. The sections were washed and incubated in detection buffer containing 100 mM Tris–HCl and 100 mM NaCl at pH 9.5. The color development was carried out using NBT/BCIP substrates (Roche, Mannheim, Germany) in the dark. Finally, the reactions were stopped by adding a buffer containing 10 mM Tris–HCl and 1 mM EDTA, pH 8.0. The sections were mounted in 90% glycerol in PBS, observed under a Nikon E600 light microscope and photographed by a Nikon DXM 1200E digital camera (Japan). Cell proliferation (the number of BrdU labeled cells) in each group was estimated in a 1-mm^2 area by using ImageJ software (1.46r).

Statistical analyses

The prawns' weights, gonadosomatic index (GSI) and cell proliferation in different groups at the same period of sampling were compared and analyzed by two-way analysis of variance (ANOVA) using the software GraphPad Prism 5 and P values were considered to be statistically significant.

Results

Immunohistochemical detection of Mro-NPF-I in the ventral nerve cord

The ventral nerve cord (VNC) of *M. rosenbergii* lying along the mid-ventral line of the body of the prawn consists of three

major parts: a fused subesophageal ganglion (SEG), five pairs of thoracic ganglia (TG) and six pairs of abdominal ganglia (AG). In this study, we performed the immunochemical detection of Mro-NPF-I immunoreactivity (Mro-NPF-I-ir) in the SEG, TG and AG whose organizations are composed of neuropils and associated neuronal clusters, which are schematically illustrated in Figs. 2a, 4a, and 6a. The histology of subesophageal ganglion (SEG) was shown by horizontal sections stained with hematoxylin and eosin (H&E) in Fig. 2. The SEG is connected anteriorly to the tritocerebrum by a pair of circumesophageal connectives (CEC) that contain nerve bundles (Fig. 2d, e). The SEG consists of mandibular or visceral sensory neuropils (VSN) and five pairs of fused neuropils called the first maxillary neuropil (MX-I), second maxillary neuropil (MX-II), first maxilliped neuropil (MP-I), second maxilliped neuropil (MP-II) and third maxilliped neuropil (MP-III) and associated neuronal clusters, namely, dorsolateral cluster (DLC) located at the periphery of the dorsomedial region and the ventromedial cluster (VMC) at the center of the ventromedial region of the SEG (Fig. 2f, g). Moreover, the SEG contains several nerve fibers supplying the first and second maxilla and the first, second and third maxilliped (Fig. 2c).

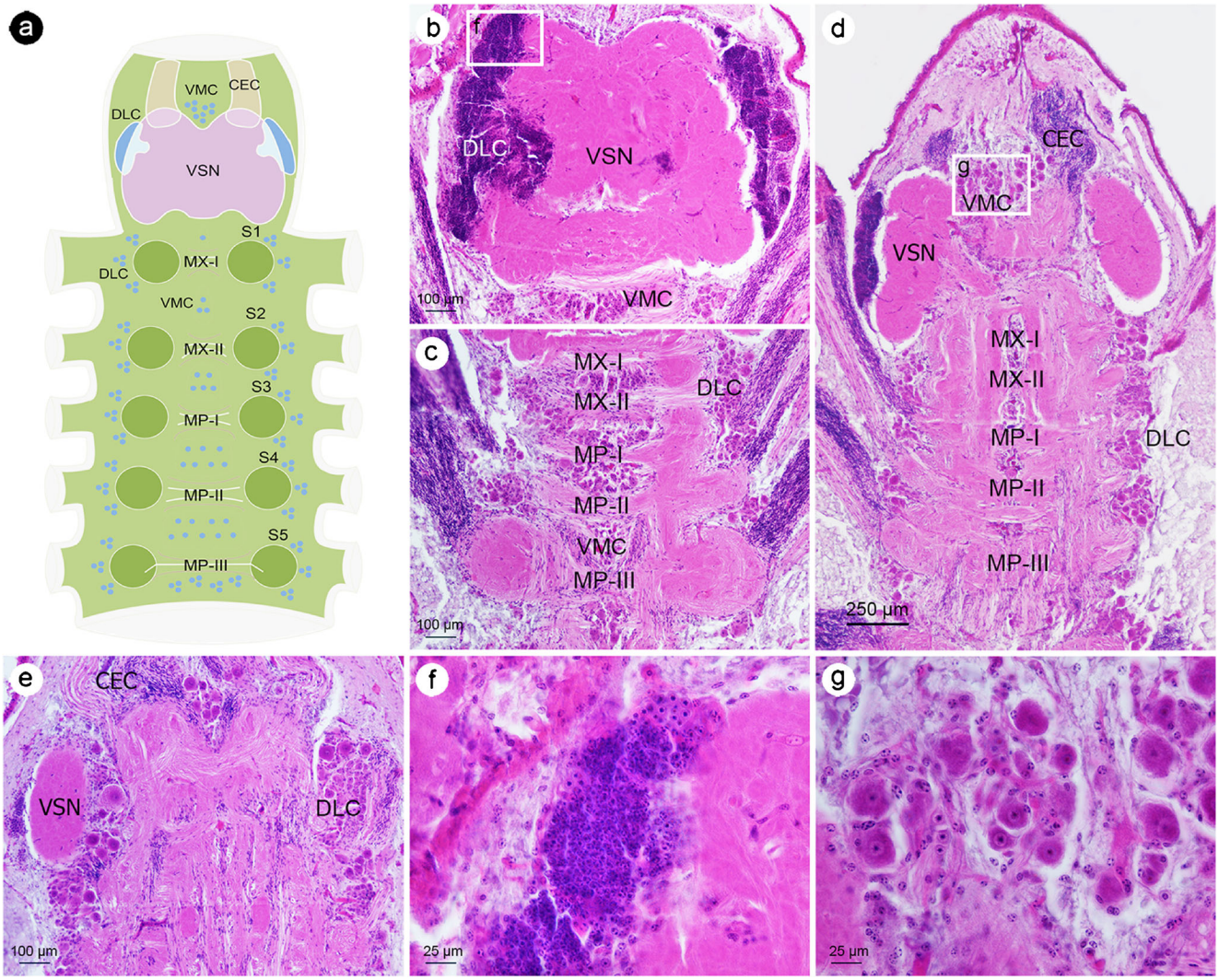

Fig. 2 Horizontal sections of subesophageal ganglion (SEG) of *M. rosenbergii* stained with hematoxylin and eosin showing the organization of neuronal cell clusters and neuropils. **a** A schematic diagram of a horizontal mid-section of SEG illustrating the organization and locations of neuronal clusters (DLC and VMC) and associated neuropils. **b**, **c** Dorsal plane sections of SEG showing mandibular or VSN and MX-I to MP-III neuropils and associated neuronal clusters, i.e., dorsolateral cluster (DLC) and ventromedial cluster (VMC). **d** Middle plane section of SEG showing VSN, MX-I to MP-III neuropils and the two neuronal clusters (DLC and VMC). **e** Ventral plane section of SEG showing a small left part of VSN and a part of DLC containing large- and medium-sized neurons. **f** High magnification of DLC of the SEG (from boxed area in **b**) containing only small neurons. **g** The VMC (from boxed area in **d**) containing medium- and large-sized neurons. Abbreviations: CEC, circumesophageal connectives; VSN, visceral sensory neuropil; MX-I, MX-II, first and second maxilla; MP-I, MP-II, MP-III, first, second and third maxilliped; DLC, dorsolateral neuronal cluster; VMC, ventromedial neuronal cluster

In immunohistochemical detection, Mro-NPF-I-ir appeared as intense punctate fibers in the VSN neuropil with few positive neurons in the center (Fig. 3a). Mro-NPF-I-ir at moderate intensity was detected in DLC globuli (small-sized) cells located laterally to the VSN (Fig. 3b). Moreover, Mro-NPF-I-ir was detected in medium-sized neurons of the DLC situated among intensely stained nerve fibers of the first and second maxilla and the first, second and third maxilliped (Fig. 3c–e).

The thoracic ganglia (TG) comprise the second part of the VNC, which is connected to the SEG by associated nerve bundles (Fig. 4b). The thoracic ganglionic chain contains five pairs of thoracic neuropils (T1–T5) and associated neuronal clusters as shown in a schematic diagram of TG (Fig. 4a). Each thoracic neuropil was associated with two neuronal clusters: dorsolateral (DLC) and ventromedial (VMC) clusters that were continuous along the ventral middle area of the VNC (Fig. 4c). The sternal artery (SA) passes through the TG between T3 and T4 (Fig. 4d). The dorsal plane of TG shows numerous cells with various sizes in DLC that are located laterally to thoracic neuropils. In the middle plane, both the DLC and the VMC were also observed to be closely associated with their corresponding neuropils (Fig. 4d). The ventral plane shows mostly large neurons of the VMC (Fig. 4e). The VMC clusters of TGs contain three types of neurons and the large neurons predominate (Fig. 4f–h). In immunohistochemical detections, Mro-NPF-I-ir appeared intense in both sides of each pair of the thoracic neuropil (Fig. 5a, b). Mro-NPF-I-ir was also intense in the small-sized neurons (< 25 μm) in DLC, a few medium-sized neurons (between 25 and 50 μm) and large-sized (between 50 and 100 μm) neurons of VMC (Fig. 5c-f). In contrast, a weak immunoreactivity was detected in most medium- and large-sized neurons of VMC (Fig. 5f).

The abdominal ganglia (AG) are an abdominal chain of ganglia that are the last part of the VNC that continue caudally from TG. There are six abdominal neuropils (A1–A6) and the paired neuropil regions of each segment are fused and are associated with the DLC neuronal cluster as depicted in a schematic diagram of the AG (Fig. 6a). Horizontal sections exhibited mostly medium- and large-sized neurons as well as a few very large or giant (G) neurons (> 100 μm) located laterally to each fused abdominal neuropil (Fig. 6b–g). The VMC is absent in the AG. Intense immunoreactive punctate fibers were detected in neuropils of A1 to A6 (Fig. 7b–g). Moderately intense Mro-NPF-I-ir was detected in medium- and large-sized as well as some giant neurons of A1 to A5 (Fig. 7a). Strong Mro-NPF-I-ir was detected in a few large-

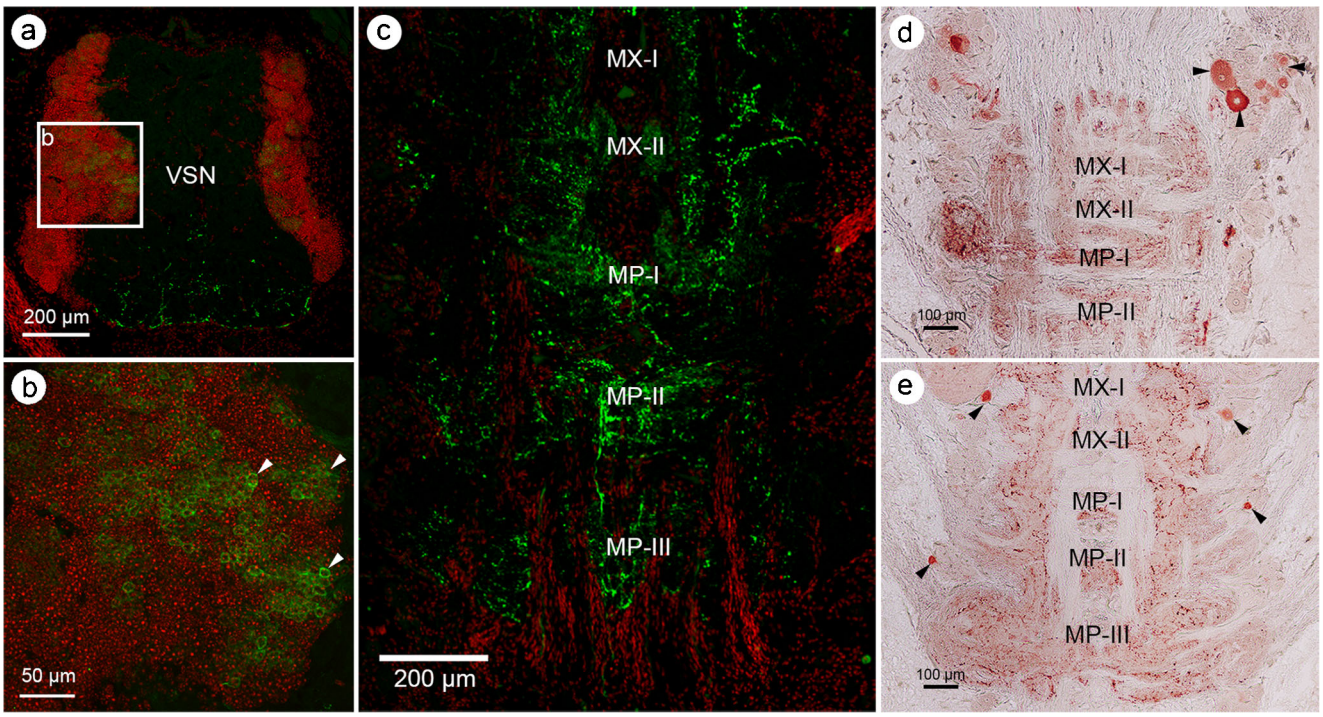

Fig. 3 Immunofluorescence detection (**a**, **b**, **c**—green) and immunoperoxidase detection (**d**, **e**—brownish red) of Mro-NPF-I-ir in SEG of *M. rosenbergii*. **a** A low-power image showing distribution of NPF-I-ir in the visceral sensory neuropil (VSN) and small neurons in the dorsolateral cluster (DLC) (boxed area). **b** A high-magnification image of DLC from the boxed area in **a**, showing Mro-NPF-I-ir in small-sized neurons indicated by white arrow heads. **c** A low-power image showing punctate appearance of the Mro-NPF-I-ir present in nerve fibers of MX-I, MX-II, MP-I, MP-II and MP-III in the middle region of SEG. **d** A medium-power image at a ventral plane showing Mro-NPF-I-ir in the DLC medium- and large-sized neurons near MX-I indicated by black arrow heads. **e** A medium-power image at the dorsal plane showing Mro-NPF-I-ir in the large DLC neurons indicated by black arrow heads. Abbreviations: VSN, visceral sensory neuropil; MX-I, MX-II, first and second maxilla; MP-I, MP-II, MP-III, first, second, and third maxilliped; DLC, dorsolateral neuronal cluster; VMC, ventromedial neuronal cluster

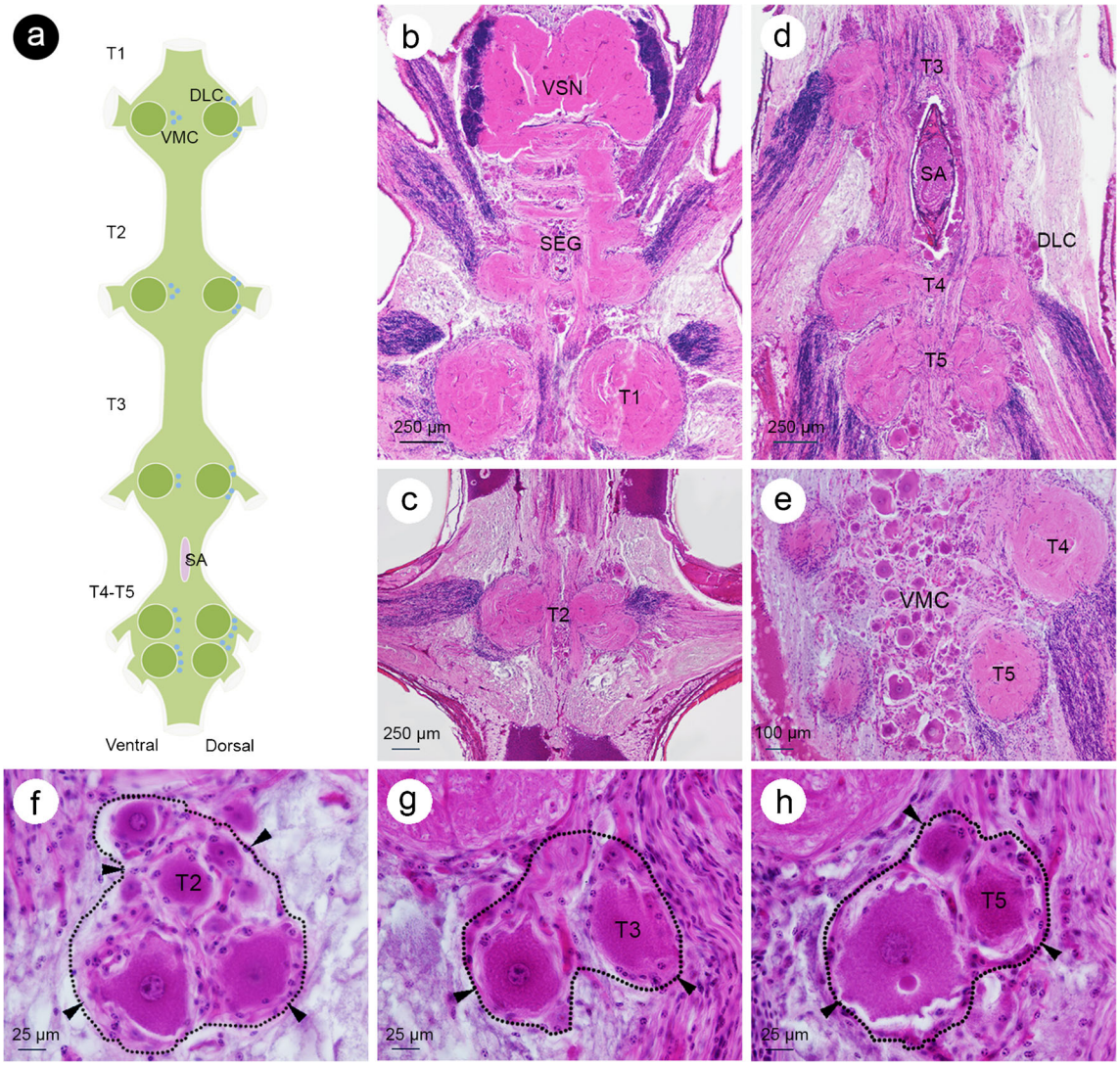

Fig. 4 Horizontal sections of thoracic ganglia (TG 1–5) of *M. rosenbergii* stained with hematoxylin and eosin, showing the organization of neuropils and associated neuronal cell clusters. **a** A schematic diagram of a mid-horizontal section of TGs illustrating the organization and locations of neuropil and neuronal clusters (DLC, VMC). **b**–**d** Low-power images of dorsal planes showing connections between SEG and T1 and T2 to T3–T5, with the sternal artery between T3 and T4. Notice the presence in DLC and VMC. **e** A medium-power image showing medium- and large-sized neurons in VMC of T4 and T5. **f**–**h** High-magnification pictures showing neurons in clusters T2, T3 and T5, which are mostly medium- and large-sized cells. Abbreviations: VSN, visceral sensory neuropil; SEG, subesophageal ganglion; T, thoracic neuropils; DLC, dorsolateral neuronal cluster; VMC, ventromedial neuronal cluster

sized neurons within A6 (Fig. 7h). Strong immunoreactivity was also detected in the fibers connecting between neuropils (Fig. 7i). The distributions of Mro-NPF-I-ir in the VNC are summarized in Table 1.

Effects of neuropeptide F on growth and testicular development

To determine the influence of Mro-NPFs on growth and testicular development, the synthetic peptides (Mro-NPF-I, Mro-sNPF) were injected into SM prawns as stated in "Materials and methods." The growth, as reflected by weight gains, from days 0 to 28 of the Mro-NPF-I-injected and Mro-sNPF-injected groups was compared with the control groups. SM prawns injected with the highest doses of Mro-NPF-I (2.5×10^{-6} mol/prawn) showed significantly increased body weight (BW) from day 12 to day 28 compared with the control groups, while Mro-sNPF-injected prawns showed a slight increase in body weights during the same period but the gains were not significantly different from the control prawns (Fig. 8). Furthermore, SM prawns injected with Mro-NPF-I and Mro-sNPF exhibited significantly increased GSI (Fig. 9). In the group injected with Mro-NPF-I at 2.5×10^{-6} mol/prawn, the GSI was increased at days 4, 8, 16 and 20 compared with the control group. As well, a significant

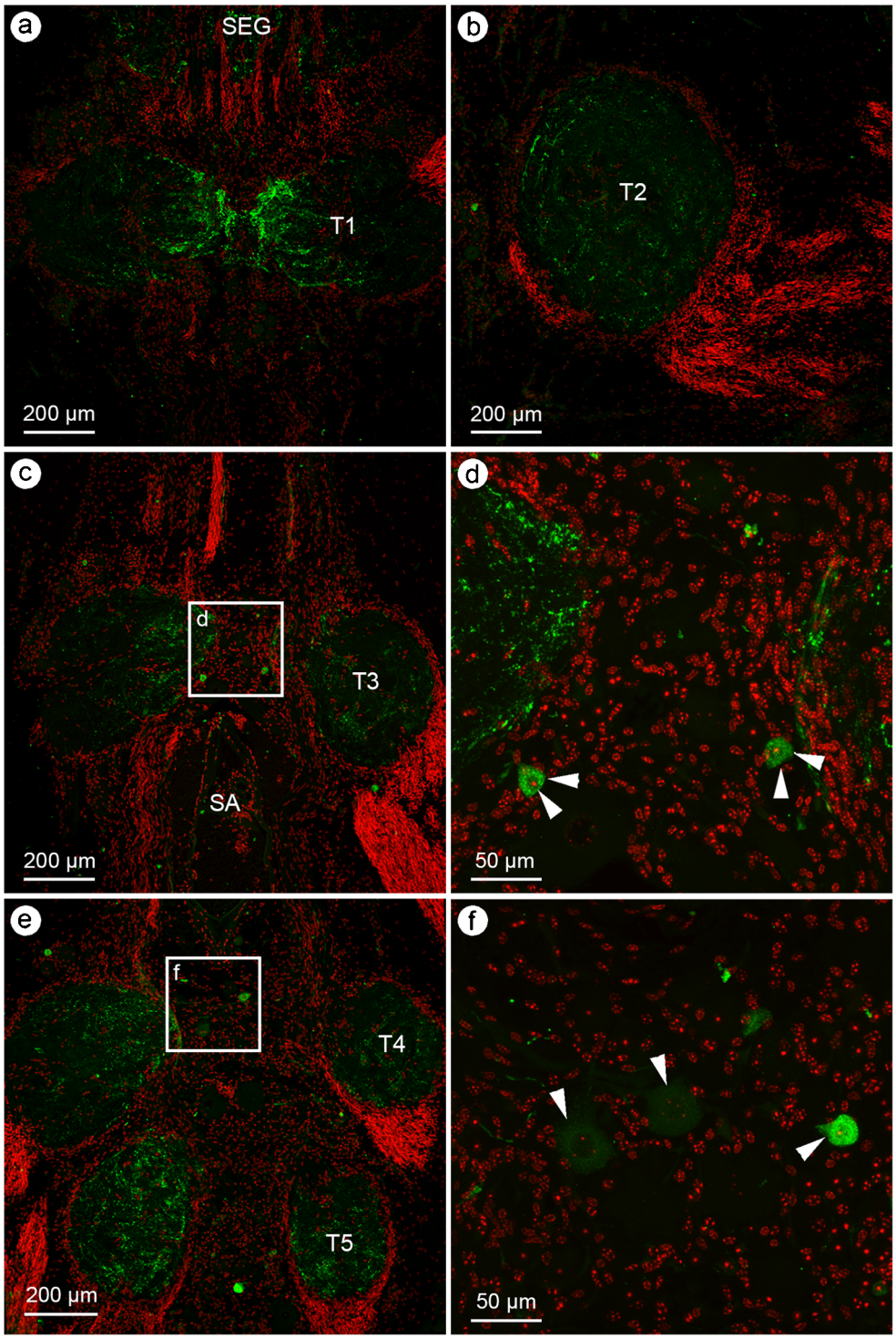

Fig. 5 Immunofluorescence detection of Mro-NPF-I-ir (green) in the TGs of *M. rosenbergii*. **a** A low-power image showing distribution of Mro-NPF-I-ir in the neuropil and VMC neuronal cluster of T1. **b** A low-power image showing distribution of Mro-NPF-I-ir in the neuropil of T2. **c**, **d** A low-power image (**c**) showing distribution of Mro-NPF-I-ir in the neuropil and a high-power image (**d**) of the boxed area in **c** displaying two positively stained medium-sized neurons in the VMC of T3. **e** A low-power image showing distribution of Mro-NPF-I-ir in the neuropils and large neurons in the VMC (boxed area) of T4 and T5. **f** A high-magnification image showing Mro-NPF-I-ir in large- and medium-sized neurons in VMC of T4 and T5 (white arrow heads). Abbreviations: SEG, subesophageal ganglion; T, thoracic neuropils

increase in GSI was observed in the group injected with Mro-NPF-I with the dose 2.5×10^{-7} mol/prawn at days 4, 8, 16 and 28 compared with the control group. The prawns injected with Mro-sNPF at 2.5×10^{-6} mol/prawn showed significantly increased GSI at days 4, 8, 12, 16 and 28 compared with the control groups, while the prawns injected with Mro-sNPF 2.5×10^{-7} mol/prawn exhibited significantly increased GSI at days 4, 8 and 12 compared with the control groups. The trend suggested that at days 20 and 24, the GSI in most groups increased more than that of the control but the difference was not significant. Overall, the data showed that Mro-NPF-I and Mro-sNPF stimulated testicular development in the male giant freshwater prawns, especially in the earliest periods examined.

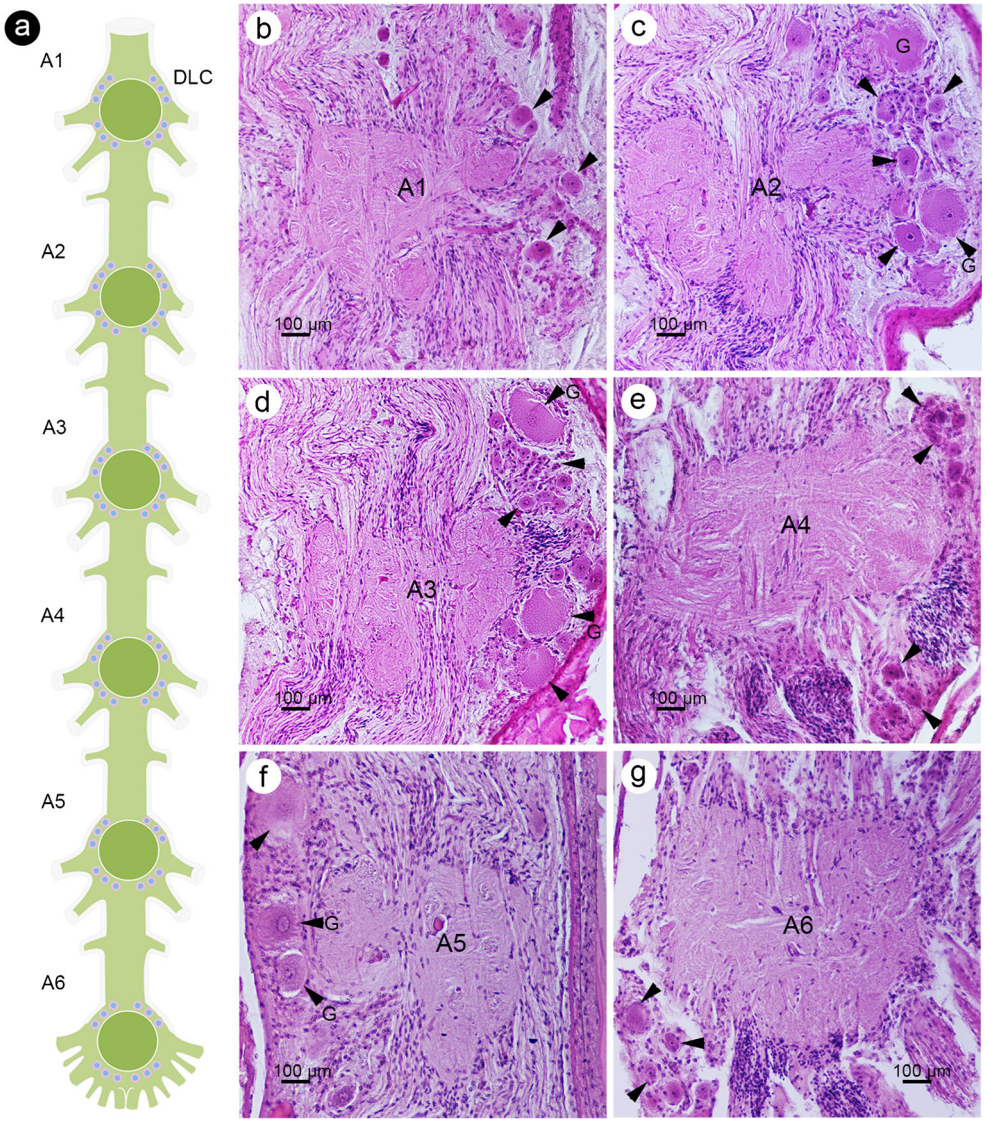

Fig. 6 Horizontal sections of abdominal ganglia (AG) of *M. rosenbergii* stained with hematoxylin and eosin, showing the organization of neuropils of AG 1 to 6 and associated DLC. **a** A schematic diagram of a mid-horizontal section of AG illustrating the organization of fused neuropils for each of the AG ganglion and associated DLC neuronal clusters. **b**, **c** Low-power images showing A1 and A2 at the dorsal plane, containing a few giant neurons as well as medium- and large-sized neurons of DLC, while there are very few neurons in VMC of A1. **d**, **e** Low-power images of A3 and A4 displaying fused neuropils and very large as well as large- and medium-sized neurons in the DLC (black arrow heads). **f**, **g** Low-power images of dorsal planes of A5 and A6 containing fused neuropils and large- as well as medium-sized neurons in the DLC (black arrow heads) of both ganglia. Abbreviations: A, abdominal neuropils; DLC, dorsolateral neuronal cluster; VMC, ventromedial neuronal cluster

The effects of neuropeptide F on testicular cell proliferation

Figure 10 depicts the numbers of BrdU-labeled nuclei per 1 mm^2 area (mean ± S.D.) of the control prawns and those treated with Mro-NPF-I and Mro-sNPF. At day 4, the seminiferous tubules of the prawns injected with Mro-NPF-I at 2.5×10^{-7} mol/prawn showed a significant increase in the number of BrdU-labeled cells compared with the control group. At day 8, the seminiferous tubules in the testes of the prawns injected with Mro-NPF-I at 2.5×10^{-6}, 2.5×10^{-7} mol/prawn and Mro-sNPF at 2.5×10^{-6} and 2.5×10^{-7} mol/prawn showed significant increases in numbers of labeled cells compared with the control group. At day 12, the cell proliferations in the seminiferous tubules of the prawns injected with Mro-sNPF exhibited a significant increase in the number of labeled cells in both groups compared with the control group. At day 16, the cell proliferation also showed a significant increase in the seminiferous tubules of the prawns injected with Mro-NPF-I at 2.5×10^{-6}, 2.5×10^{-7} mol/prawn and Mro-sNPF at 2.5×10^{-7} mol/prawn compared with the control group. Lastly, the seminiferous tubules of testes of the prawns injected with Mro-sNPF at 2.5×10^{-7} exhibited a significant increase in cell proliferation at day 20 compared with the control group. However, the differences between the treated and control groups were not significantly different at days 24 and 28. Overall, all NPF-injected groups showed significant increases in cell proliferations during the early periods between days 4 and 16 when compared to the control group.

Examples of BrdU-labeled cells were shown by examining the immunohistochemically stained cells at day 8. Histology of seminiferous tubules was displayed by H&E-stained sections (Fig. 11a), which showed mostly tubules in stage VIII and each tubule contained a crescentic compact area where labeled cells resided and these were early germ cells (mostly

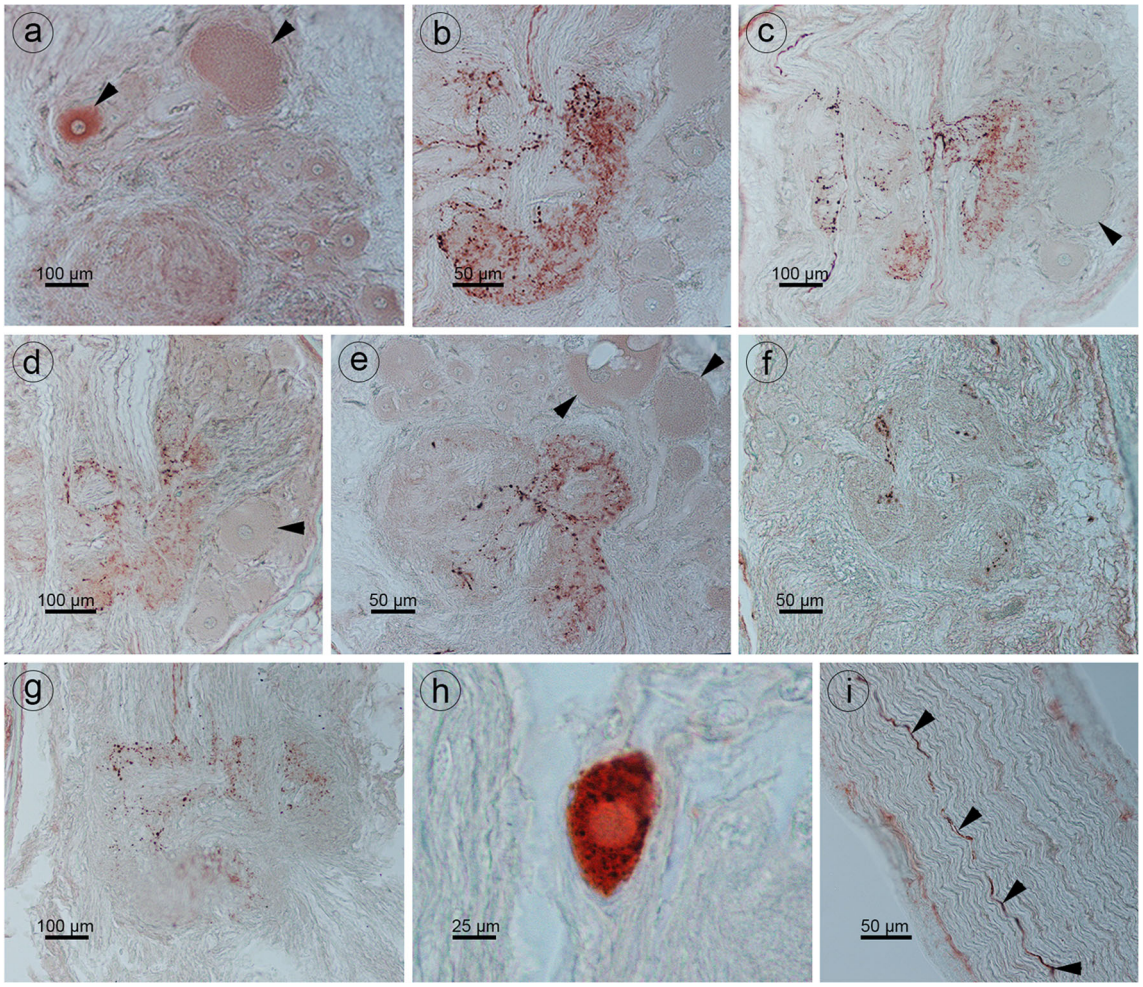

Fig. 7 Immunoperoxidase detection of Mro-NPF-I-ir in AG of *M. rosenbergii*. **a** A low-power image showing Mro-NPF-I-ir in the neuropil and both large and giant neurons of A1 (arrow heads indicate a large neuron at the left side and giant neurons at the right side). **b** A medium-power image showing distribution of strong NPF-I-ir in the neuropil of A1. **c**, **d** Low-power images showing distribution of NPF-I-ir in the neuropils of A2 and A3, respectively, and large neurons of these regions are also lightly stained (black arrow heads). **e**, **f** Medium-power images showing distribution of NPF-I-ir in the neuropils of A4 and A5, respectively and large neurons in the E region are also lightly stained (black arrow heads). **g** A medium-power image showing distribution of Mro-NPF-I-ir in the neuropil of A6. **h** A high-magnification image showing intense Mro-NPF-I-ir, a large neuron of A6. **i** A medium-power image showing NPF-I-ir in connecting fibers between A1 and A2

spermatogonia and early spermatocytes), while the remaining looser area contained mainly spermatozoa. Thus, most if not all of the labeled cells were early germ cells and not spermatozoa. The prawns injected with 0.1 M PBS showed only few positively labeled cells in this area in contrast to Mro-NPF-injected groups (Fig. 11b–f).

Discussion

In the present study, we documented the distribution of Mro-NPF-I in the ventral nerve cord (VNC) and examined the role of Mro-NPF-I and Mro-sNPF on the development of testes in small male *M. rosenbergii*. We found that the rabbit polyclonal antibody against Mro-NPF-I could detect Mro-NPF-I immunoreactivity (ir) in the neuropils and cell clusters of the subesophageal ganglion (SEG), thoracic ganglia (TG) and abdominal ganglia (AG). In addition, administrations of synthetic Mro-NPF-I and MrsNPF peptides significantly increased the gonadosomatic index (GSI) and cell proliferations in the seminiferous tubules of testes in small male giant freshwater prawns.

The neuropeptide F has been identified in several invertebrate species including tapeworm, mollusks and slug (Nassel and Wegener 2011). In crustaceans, NPF isoforms have been identified in the water flea, *Daphnia pulex*, using transcriptomic analyses (Gard et al. 2009). Subsequently, NPFs were characterized in penaeid shrimps *Litopenaeus vannamei* and *Melicertus marginatus* by reverse transcription-polymerase chain reaction (RT-PCR) (Christie et al. 2011). Moreover, the short NPF (sNPF) has been isolated in Colorado potato beetles, *Leptinotarsa decemlineata* (Spittaels et al. 1996) and their

Table 1 Distribution of Mro-NPF-ir in the VNC of *M. rosenbergii*: +++ strong immunoreactivity, ++ moderate immunoreactivity, + weak immunoreactivity, − no immunoreactivity, VNC - ventral nerve cord, SEG - subesophageal ganglion, TG - thoracic ganglion, CEC - circumesophageal connectives, VSN - visceral sensory neuropil, DLC- dorsolateral neuronal cluster, VMC - ventromedial neuronal cluster, S - small-sized neuron, M - medium-sized neuron, L - large-sized neuron, G - giant-sized neuron, NF - neural fibers

Structure	Regions	Neuronal cluster/neuropils	Type of neurons/fibers	MrNPF-ir intensity
VNC	SEG	CEC	NF	+
		Mandibular (VSN)	NF	++
		Maxilla I–II	NF	++
		Maxilliped I–III	NF	++
		VMC	M, L	+
		DLC	S, M, L	++
	TG	T1 neuropil	NF	++
		VMC/DLC	M, L	+
		T2 neuropil	NF	++
		VMC/DLC	M, L	+
		T3 neuropil	NF	++
		VMC/DLC	M, L	++
		T4 neuropil	NF	+++
		VMC/DLC	M, L	++
		T5 neuropil	NF	+++
		VMC/DLC	M, L	++
	AB	A1 neuropil	NF	+++
		DLC	M, L, G	++
		A2 neuropil	NF	+++
		DLC	M, L, G	++
		A3 neuropil	NF	+++
		DLC	M, L, G	++
		A4 neuropil	NF	+++
		DLC	M, L, G	++
		A5 neuropil	NF	+++
		DLC	M, L, G	++
		A6 neuropil	NF	+++
		DLC	M, L, G	++

sequences are ARGPQLRLRF-NH_2 and APSLRLRF-NH_2 peptides. Recently, by transcriptomic analyses, our group found three isoforms of NPFs and four isoforms of sNPF in the female prawns, *Macrobrachium rosenbergii*. NPFs were identified as Mro-NPF-I, Mro-NPF-II and Mro-NPF-III whose genes were detected in the transcriptomes of the eyestalk, CNS and ovary. The sNPF transcript was also detected from the eyestalk and CNS and gives rise to four active peptides. Moreover, by RT-PCR, we found that Mro-NPF-I was expressed in several tissues including eyestalk, brain, thoracic ganglia, abdominal ganglia, testis, heart and muscle (Suwansa-Ard et al. 2015). NPFs were also shown to be generally expressed in the neural tissues of other invertebrate species. In the insect, *D. melanogaster*, NPF is expressed in the central nervous system, including the lateral protocerebrum of the brain and subesophageal ganglion (Nagata 2016). In mollusks, NPF-ir has been detected in the cerebral ganglion and subesophageal ganglion of *Helix aspersa* by immunogold labeling and immunofluorescence (Leung et al. 1994a, b). The tissue distribution of NPF in decapod crustaceans had been first described by our group in *M. rosenbergii*, where NPF-I was detected in parts of the brain that include the neuropils and neuronal clusters in the protocerebrum, deutocerebrum and tritocerebrum (Thongrod et al. 2017). In this study, we extended the investigation on NPF tissue distribution in all parts of the ventral nerve cord (VNC), which includes SEG, TG and AG. Mro-NPF-I was found in the VMC, DLC neurons, punctuate fibers in VSN neuropil of the SEG and associated nerve fibers of the SEG that innervate the mandibles, maxillae and maxillipeds that control the movements of the mouth parts. The presence of generally intense Mro-NPF-I-ir in these structures implies that NPF could be involved in feeding and could also indicate its role in gill ventilation (Pasztor 1968; Wilkens 1976). In addition, Mro-NPF-I-ir was also detected in medium-sized neurons of DLC and VMC of TGs and associated neuropils. TGs give rise to nerve-innervating muscles of the first and second chelipeds as well as the walking legs (Harzsch 2003; Harzsch et al. 1998). Moreover, Mro-NPF-I-ir was also detected in all neuropils and some large and giant neurons of the AG, implicating that they may have control over the swimmerets and tail movement in this prawn. In adult *Drosophila*, gustatory receptor neurons (GRNs) are found in the distal lobes of the mouth parts. GRNs send their axons to distinct subregions of the primary gustatory center (PGC) in the subesophageal ganglion (SEG). After receiving input from the GRNs, second-order gustatory neurons project their fibers to form synapses in the distal brain region adjacent to the SEG. These secondary gustatory projection neurons participate in controlling feeding behaviors as they send information about taste, which is processed by neural circuitry within the SEG before it is sent further into the brain. In addition, the SEG also integrates sensory information with motor nerves that innervate the neck and mouth parts (Miyazaki et al. 2015). In arthropods, thoracic ganglia next to the SEG also contain neurons controlling the movement of appendages that includes pattern-generating interneurons and motor neurons that innervate the appendage muscles (Elson 1996; Smarandache-Wellmann 2016). In the crayfish, *Procambarus clarkii*, some neurons in abdominal ganglia send fibers directly to the intestine and hindgut (Johansson and Schmidt 1997; Kondoh and Hisada 1986; Reichert et al. 1982). Moreover, the nerve fibers extending from each abdominal neuropil join to form abdominal nerves that supply the pleopods or swimmerets of the abdominal region (Saetan et al. 2013; Smarandache-Wellmann 2016). Therefore, we suggested that NPF present in the SEG and TG may coordinate the motor activities of the mouth parts in the food handling and the

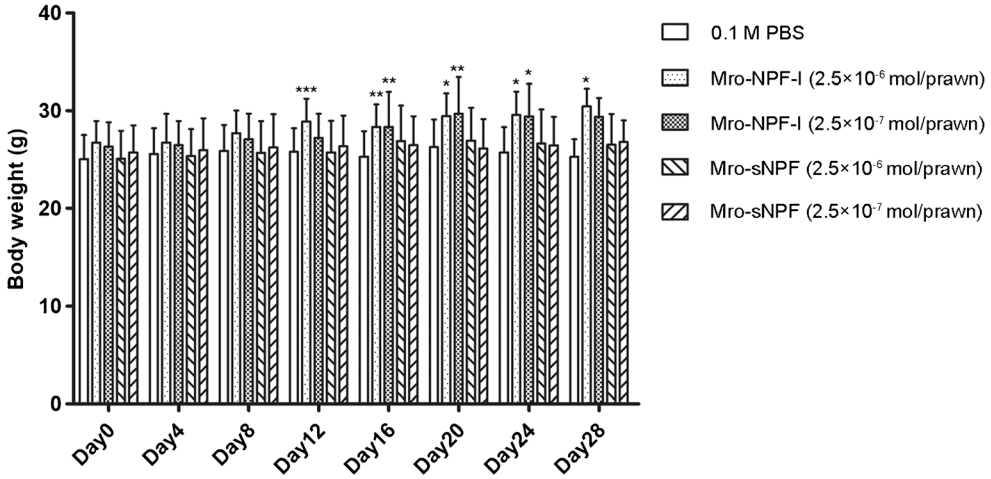

Fig. 8 The effects of Mro-NPF-I and Mro-sNPF on growth of small males *M. rosenbergii* as displayed by the averages of body weights (BW). Each treatment is defined by the peptides' names and doses, i.e., Mro-NPF-I at doses of 2.5×10^{6} and 2.5×10^{-7} mol/prawn and Mro-sNPF at doses of 2.5×10^{-6} and 2.5×10^{-7} mol/prawn. BW values (in grams) of prawns injected with Mro-NPF-I and Mro-sNPF compared to the control group injected with PBS from days 4 to 28, showing significant increases in the BW of the groups injected with Mro-NPF-I from days 12 to 28, when compared to the PBS-injected control group (*$P < 0.05$; **$P < 0.01$; ***$P < 0.001$)

movements of the walking legs to synchronize the food-finding activity guided by gustatory and olfactory inputs, so that the prawns can directionally move towards the food to begin foraging and feeding (Corotto et al. 1992; Derby and Atema 1982; Voigt and Atema 1992). Moreover, the detection of Mro-NPF-I-ir in neuropils and most neuronal clusters of AG suggests that NPF could be involved in the coordinated movement of the swimmerets, the tail, intestine and hindgut.

Functionally, the classical roles of NPFs are demonstrated to be controls of feeding behavior, foraging and stress responses (Nassel and Wegener 2011). In insects, the injection of truncated form NPF (YSQVARPRF-NH_2) stimulated food intake and increased body weight of the desert locust, *Schistocerca gregaria* (Van Wielendaele et al. 2013a). In crustaceans, it was also shown that NPF is involved in feeding by increasing the food intake and body weight in juvenile *L. vannamei* after being fed with NPF-I-mixed feed (KPD PSQLANMAEALKYLQELDKYYSQVSRPRFamide) compared to the control group (Christie et al. 2011). Recently, our group found that starvation in female *M. rosenbergii* could induce autophagy and stimulate ovarian maturation (Kankuan et al. 2017). In the most recent study, we found that Mro-NPF-I could stimulate autophagy in the hepatopancreas and muscle, which are the reserve organs for the nutrient homeostasis during starvation (Thongrod et al. 2018). Taken together, these studies showed a strong linkage between NPF, autophagy and gonadal development.

The male prawns can be classified into three morphotypes (Kuris et al. 1987; Ranjeet and Kurup 2002). The first are small males (SM) that are developed from juvenile prawns. The second stage includes orange claw males (OC) that have gold-colored second pereiopods (chelipeds) and are

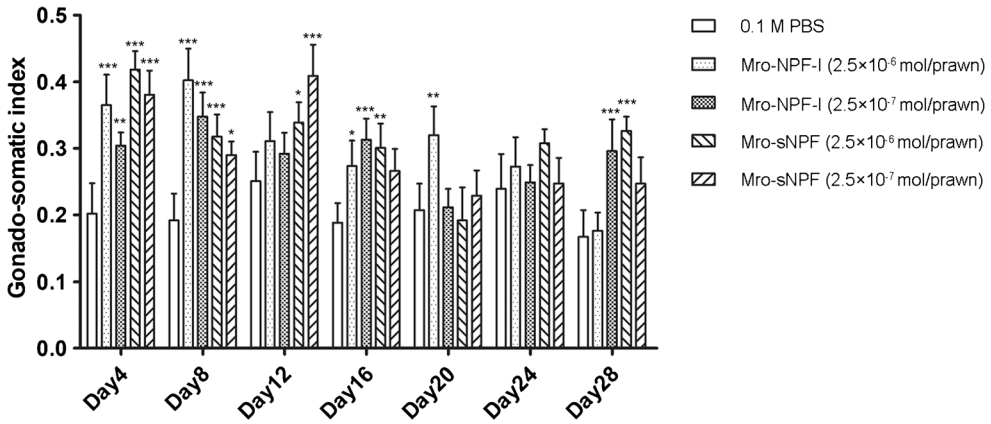

Fig. 9 Gonadosomatic index (GSI) of prawns injected with Mro-NPF-I and Mro-sNPF compared to the control group injected with PBS from days 4 to 28, showing significant increases in the GSI of groups injected with Mro-NPF-I and Mro-sNPF from days 4 to 16 when compared to the PBS-injected control group (*$P < 0.05$; **$P < 0.01$; ***$P < 0.001$). However, there were some increases of the GSI but mostly with no significant difference from the control at days 20 and 24

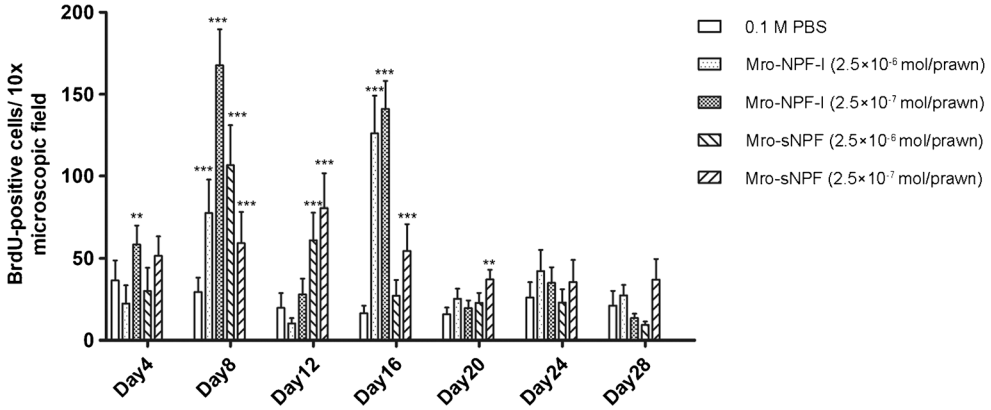

Fig. 10 The effects of Mro-NPF-I and Mro-sNPF on germ cell proliferation in testes of small males *M. rosenbergii* as estimated by the numbers of BrdU-labeled nuclei ($N = 6$) per square millimeter. Histograms showing mean ± S.D. of BrdU-labeled nuclei per 1-mm^2 area. There were significantly more BrdU-labeled cells in the testes of Mro-NPF-I- and Mro-sNPF-injected prawns at days 4 to 16 when compared to the PBS-injected control group (*$P < 0.05$; **$P < 0.01$; ***$P < 0.001$). Thereafter, the differences were mostly not significant

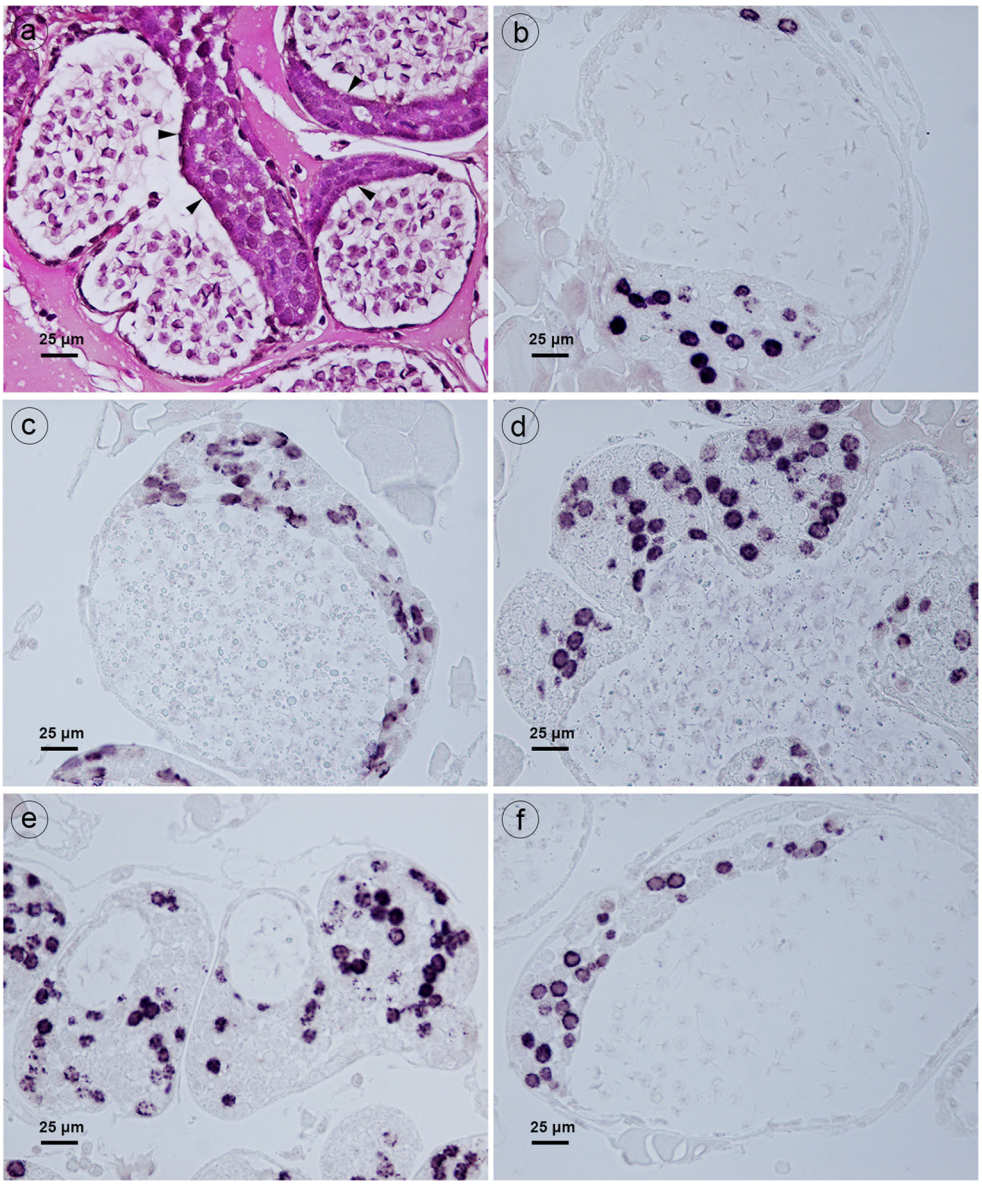

Fig. 11 Examples of BrdU-labeled nuclei examined at day 8. **a** Seminiferous tubules of a control prawn injected with 0.1 M PBS and stained with hematoxylin and eosin, showing that early germ cells (spermatogonia and spermatocytes) are tightly packed together in the crescentic area at one edge of each tubule (arrow heads) while spermatozoa are loosely packed in the remaining area. **b** The testis of a control prawn showing few BrdU-labeled cells. **c** The testis of a prawn injected with Mro-NPF-I at a dose 2.5×10^{-6} mol/prawn. **d** The testis of a prawn injected with Mro-NPF-I at a dose 2.5×10^{-7} mol/prawn. **e** The testis of a prawn injected with Mro-sNPF at a dose 2.5×10^{-6} mol/prawn. f. The testis of a prawn injected with Mro-sNPF at a dose 2.5×10^{-7} mol/prawn. All of the NPF-injected groups showed more BrdU-labeled cells than the PBS-injected control group

transformed from SM. The last are blue claw males (BC) that are the largest and have the longest blue claws and they also develop from OC males. Usually, in mixed culture, SM do not reach full maturity as they are suppressed by a more dominating and aggressive behavior of BM, perhaps through the release of pheromones. Likewise, the development of their testes is arrested at early stages in which there are few fully developed spermatozoa (Poljaroen et al. 2011). If SM are freed from BM or cultured alone, they rapidly increase in size and their testes become fully functional. Several studies showed that neurotransmitters and hormones from the CNS (possibly GSH or GnRH-like factors) and a hormone from the androgenic gland (insulin-like androgenic gland hormone (IAGH)) could stimulate testicular development and spermatogenesis in SM prawns (Poljaroen et al. 2011; Siangcham et al. 2013). Here, we found that both a long (Mro-NPF-I) and a short Mro-NPF, neuropeptides classically considered linking more to feeding, could also stimulate testicular development and proliferation of male germ cells in the SM prawns.

In the present study, synthetic Mro-NPF-I and Mro-sNPF were used to test for effects on growth as well as testicular development in the SM prawns. We found that the body weight of NPF-treated groups was significantly increased only in Mro-NPF-I-injected groups but not in Mro-sNPF-injected groups perhaps because the experimental period was too short (only 28 days). GSI levels, however, were significantly increased after injections in both Mro-NPF-I and Mro-sNPF-injected groups, especially during the early period of the experiment. The gonadotrophic effect of NPFs was quite surprising to us initially. However, a previous study showed that female desert locusts injected with an NPF nanopeptide (YSQVARPRF-NH_2) showed increased ovarian development and oocyte enlargement (Van Wielendaele et al. 2013b). Moreover, NPF administration also increased the weight of the testis and seminal vesicle in the male locust (Van Wielendaele et al. 2013c). Recently, our group reported that Mro-NPF-I stimulated the ovarian maturation and spawning in the female *M. rosenbergii* (Tinikul et al. 2017). In the present study, we further found that both Mro-NPF-I and Mro-sNPF injections showed significant increases in the testicular cell proliferations in the seminiferous tubules using BrdU labeling and that most of the dividing cells were located in the proliferative (compact) zone of the tubules where early germ cells, including spermatogonia and spermatocytes, were concentrated. In contrast, the BrdU labels were absent in the looser parts (lumen) of the tubules that contain late spermatids and spermatozoa.

In conclusion, we detected the Mro-NPF-I immunoreactivity, implicating the tissue expression of Mro-NPF-I, in the neuropils and associated neuronal clusters of subesophageal, thoracic and abdominal ganglia, in addition to parts of the brain as reported earlier (Thongrod et al. 2017). Furthermore, both Mro-NPF-I and one isoform of Mro-sNPF also positively affected the testicular development and germ cell proliferation in SM prawns. In future study, we would like to investigate the distribution of Mro-NPF-I in other organs involved in reproduction and feeding, especially the testis and parts of the digestive tract. As well, a longer period of experiment should be trialed so that long-term effects of NPFs on feeding, growth and testicular maturation and transformation of SM prawns to the more mature stages can be ascertained, which will benefit the aquaculture of this species.

Acknowledgments We extend our gratitude to Capt. Piyachat Chansela, Dr. Morakot Sroyraya, Dr. Thanapong Kruangkum and Ms. Sineenart Songkoomkrong for their suggestions and technical advices.

Funding information This research was supported by a grant from the Office of Higher Education Commission (OHEC) and Mahidol University (MU) under the National Research University Initiatives and an OHEC-MU-Thailand Research Fund (TRF) Distinguished Research Professor Grant to Prasert Sobhon. This study was also supported by the Thailand Research Fund—the Royal Golden Jubilee Ph.D. Programme (TRF-RGJ Ph.D., PHD/0093/2553) co-funded by Mahidol University to Chaitip Wanichanon and Sirorat Thongrod and by National Research Council of Thailand (NRCT) scholarship (2016) to Sirorat Thongrod.

Compliance with ethical standards

All the treatment protocols were carried out according to the guidelines set by the Ethic Committee on the Use of Experimental Animals, Faculty of Science, Mahidol University.

References

Carlsson MA, Enell LE, Nassel DR (2013) Distribution of short neuropeptide F and its receptor in neuronal circuits related to feeding in larval Drosophila. Cell Tissue Res 353(3):511–523. https://doi.org/10.1007/s00441-013-1660-4

Christie AE, Cashman CR, Brennan HR, Ma M, Sousa GL, Li L et al (2008) Identification of putative crustacean neuropeptides using in silico analyses of publicly accessible expressed sequence tags. Gen Comp Endocrinol 156(2):246–264. https://doi.org/10.1016/j.ygcen.2008.01.018

Christie AE, Chapline MC, Jackson JM, Dowda JK, Hartline N, Malecha SR et al (2011) Identification, tissue distribution and orexigenic activity of neuropeptide F (NPF) in penaeid shrimp. J Exp Biol 214(Pt 8):1386–1396. https://doi.org/10.1242/jeb.053173

Corotto F, Voigt R, Atema J (1992) Spectral tuning of chemoreceptor cells of the third maxilliped of the lobster, Homarus americanus. Biol Bull 183(3):456–462. https://doi.org/10.2307/1542022

Derby CD, Atema J (1982) Chemosensitivity of walking legs of the lobster Homarus Americanus: neurophysiological response spectrum and thresholds. J Exp Biol 98(1):303–315

Elson RC (1996) Neuroanatomy of a crayfish thoracic ganglion: sensory and motor roots of the walking-leg nerves and possible homologies with insects. J Comp Neurol 365(1):1–17. https://doi.org/10.1002/(SICI)1096-9861(19960129)365:1<1::AID-CNE1>3.0.CO;2-7

Gard AL, Lenz PH, Shaw JR, Christie AE (2009) Identification of putative peptide paracrines/hormones in the water flea Daphnia pulex

(Crustacea; Branchiopoda; Cladocera) using transcriptomics and immunohistochemistry. Gen Comp Endocrinol 160(3):271–287. https://doi.org/10.1016/j.ygcen.2008.12.014

Harzsch S (2003) Ontogeny of the ventral nerve cord in malacostracan crustaceans: a common plan for neuronal development in Crustacea, Hexapoda and other Arthropoda? Arthropod Struct Dev 32(1):17–37. https://doi.org/10.1016/S1467-8039(03)00008-2

Harzsch S, Miller J, Benton J, Dawirs RR, Beltz B (1998) Neurogenesis in the thoracic neuromeres of two crustaceans with different types of metamorphic development. J Exp Biol 201(Pt 17):2465–2479

Johansson KUI, Schmidt M (1997) Dopaminergic modulation of spontaneous activity in the brain of the crayfish Cherax destructor (Decapoda, Crustacea). Can J Zool 75(1):18–26. https://doi.org/10.1139/z97-003

Kankuan W, Wanichanon C, Titone R, Engsusophon A, Sumpownon C, Suphamungmee W et al (2017) Starvation promotes autophagy-associated maturation of the ovary in the giant freshwater prawn, Macrobrachium rosenbergii. Front Physiol 8(300):300. https://doi.org/10.3389/fphys.2017.00300

Karl T, Herzog H (2007) Behavioral profiling of NPY in aggression and neuropsychiatric diseases. Peptides 28(2):326–333. https://doi.org/10.1016/j.peptides.2006.07.027

Kondoh Y, Hisada M (1986) Neuroanatomy of the terminal (sixth abdominal) ganglion of the crayfish, Procambarus clarkii (Girard). Cell Tissue Res 243(2):273–288. https://doi.org/10.1007/bf00251041

Kuris AM, Ra'anan Z, Sagi A, Cohen D (1987) Morphotypic differentiation of male Malaysian giant prawns, Macrobrachium Rosenbergii. J Crustac Biol 7(2):219–237. https://doi.org/10.2307/1548603

Leung PS, Brennan GP, Halton DW, Shaw C, Maule AG, Irvine GB (1994a) Immunocytochemical localization of neuropeptide F-immunoreactivity in the circumoesophageal ganglia of the gastropod mollusc, Helix aspersa using electron microscopy. Tissue Cell 26(1):115–122. https://doi.org/10.1016/0040-8166(94)90087-6

Leung PS, Shaw C, Johnston CF, Irvine GB (1994b) Immunocytochemical distribution of neuropeptide F (NPF) in the gastropod mollusc, Helix aspersa, and in several other invertebrates. Cell Tissue Res 275(2):383–393

Miyazaki T, Lin TY, Ito K, Lee CH, Stopfer M (2015) A gustatory second-order neuron that connects sucrose-sensitive primary neurons and a distinct region of the gnathal ganglion in the Drosophila brain. J Neurogenet 29(2–3):144–155. https://doi.org/10.3109/01677063.2015.1054993

Nagata S (2016) Chapter 41— neuropeptide F A2—Takei, Yoshio. In: Ando H, Tsutsui K (eds) Handbook of hormones. Academic Press, San Diego, pp 355–356

Nassel DR, Wegener C (2011) A comparative review of short and long neuropeptide F signaling in invertebrates: any similarities to vertebrate neuropeptide Y signaling? Peptides 32(6):1335–1355. https://doi.org/10.1016/j.peptides.2011.03.013

Pasztor VM (1968) The neurophysiology of respiration in decapod crustacea. I The motor system. Can J Zool 46(3):585–596

Poljaroen J, Tinikul Y, Phoungpetchara I, Kankoun W, Suwansa-ard S, Siangcham T et al (2011) The effects of biogenic amines, gonadotropin-releasing hormones and corazonin on spermatogenesis in sexually mature small giant freshwater prawns, Macrobrachium rosenbergii (De Man, 1879). Aquaculture 321(1):121–129. https://doi.org/10.1016/j.aquaculture.2011.08.022

Ranjeet K, Kurup B (2002) Heterogeneous individual growth of Macrobrachium rosenbergii male morphotypes. NAGA 25(2):13–18

Reichert H, Plummer MR, Hagiwara G, Roth RL, Wine JJ (1982) Local interneurons in the terminal abdominal ganglion of the crayfish. J Comp Physiol 149(2):145–162. https://doi.org/10.1007/bf00619210

Roller L, Yamanaka N, Watanabe K, Daubnerova I, Zitnan D, Kataoka H et al (2008) The unique evolution of neuropeptide genes in the silkworm Bombyx mori. Insect Biochem Mol Biol 38(12):1147–1157. https://doi.org/10.1016/j.ibmb.2008.04.009

Rungsin W, Paankhao N, Na-Nakorn U (2006) Production of all-male stock by neofemale technology of the Thai strain of freshwater prawn, Macrobrachium rosenbergii. Aquaculture 259(1):88–94. https://doi.org/10.1016/j.aquaculture.2006.05.041

Saetan J, Senarai T, Tamtin M, Weerachatyanukul W, Chavadej J, Hanna PJ et al (2013) Histological organization of the central nervous system and distribution of a gonadotropin-releasing hormone-like peptide in the blue crab, Portunus pelagicus. Cell Tissue Res 353(3):493–510. https://doi.org/10.1007/s00441-013-1650-6

Siangcham T, Tinikul Y, Poljaroen J, Sroyraya M, Changklungmoa N, Phoungpetchara I et al (2013) The effects of serotonin, dopamine, gonadotropin-releasing hormones, and corazonin, on the androgenic gland of the giant freshwater prawn, Macrobrachium rosenbergii. *Gen Comp Endocrinol 193*(supplement C):10–18. https://doi.org/10.1016/j.ygcen.2013.06.028

Smarandache-Wellmann CR (2016) Arthropod neurons and nervous system. Curr Biol 26(20):R960–R965. https://doi.org/10.1016/j.cub.2016.07.063

Spittaels K, Verhaert P, Shaw C, Johnston RN, Devreese B, Van Beeumen J et al (1996) Insect neuropeptide F (NPF)-related peptides: isolation from Colorado potato beetle (Leptinotarsa decemlineata) brain. Insect Biochem Mol Biol 26(4):375–382

Suwansa-Ard S, Thongbuakaew T, Wang T, Zhao M, Elizur A, Hanna PJ et al (2015) In silico neuropeptidome of female Macrobrachium rosenbergii based on transcriptome and peptide mining of eyestalk, central nervous system and ovary. PLoS One 10(5):e0123848. https://doi.org/10.1371/journal.pone.0123848

Thongrod S, Changklungmoa N, Chansela P, Siangcham T, Kruangkum T, Suwansa-Ard S et al (2017) Characterization and tissue distribution of neuropeptide F in the eyestalk and brain of the male giant freshwater prawn, Macrobrachium rosenbergii. Cell Tissue Res 367(2):181–195. https://doi.org/10.1007/s00441-016-2538-z

Thongrod S, Wanichanon C, Kankuan W, Siangcham T, Phadngam S, Morani F et al (2018) Autophagy-associated shrinkage of the hepatopancreas in fasting male Macrobrachium rosenbergii is rescued by neuropeptide F. Front Physiol 9:613. https://doi.org/10.3389/fphys.2018.00613

Tinikul Y, Engsusophon A, Kruangkum T, Thongrod S, Tinikul R, Sobhon P (2017) Neuropeptide F stimulates ovarian development and spawning in the female giant freshwater prawn, Macrobrachium rosenbergii, and its expression in the ovary during ovarian maturation cycle. *Aquaculture 469*(Supplement C):128–136. https://doi.org/10.1016/j.aquaculture.2016.11.026

Van Wielendaele P, Dillen S, Zels S, Badisco L, Vanden Broeck J (2013a) Regulation of feeding by neuropeptide F in the desert locust, Schistocerca gregaria. Insect Biochem Mol Biol 43(1):102–114. https://doi.org/10.1016/j.ibmb.2012.10.002

Van Wielendaele P, Wynant N, Dillen S, Badisco L, Marchal E, Vanden Broeck J (2013b) In vivo effect of neuropeptide F on ecdysteroidogenesis in adult female desert locusts (Schistocerca gregaria). J Insect Physiol 59(6):624–630. https://doi.org/10.1016/j.jinsphys.2013.03.005

Van Wielendaele P, Wynant N, Dillen S, Zels S, Badisco L, Vanden Broeck J (2013c) Neuropeptide F regulates male reproductive processes in the desert locust, Schistocerca gregaria. Insect Biochem Mol Biol 43(3):252–259. https://doi.org/10.1016/j.ibmb.2012.12.004

Voigt R, Atema J (1992) Tuning of chemoreceptor cells of the second antenna of the American lobster (Homarus americanus) with a comparison of four of its other chemoreceptor organs. J Comp Physiol A 171(5):673–683. https://doi.org/10.1007/bf00194115

Wilkens JL (1976) Neuronal control of respiration in decapod crustacea. Fed Proc 35(9):2000–2006